Influence of diaphragm opening time on shock-tube flows

By DONALD R. WHITE
General Electric Research Laboratory, Schenectady, New York

(*Received* 13 *May* 1958)

SUMMARY

Shock waves generated in a shock tube by use of hydrogen or helium as a driver gas and air, nitrogen, oxygen or argon as a driven gas have higher velocities than predicted by simple theory when sufficiently large diaphragm pressure ratios are used. Expected shock-tube performance curves have been constructed using the equilibrium Hugoniot for the driven gas, both for the usual model of shock tube flow, which assumes instantaneous diaphragm removal, and for a suggested model based on a finite rupture time for the diaphragm. Agreement between experiment and the latter model is in general good, and the differences are qualitatively accounted for by the pressure waves expected to result from mixing between driver and driven gases at the contact surface. These waves may be either compression or expansion waves, depending on the relative heat capacities of the two gases. The maximum shock strength observed as a shock goes down the tube was found to occur at a distance from the diaphragm which increases with the shock strength, and the strongest shocks were found to be still accelerating at the end of a 42 ft. long shock tube of $3\frac{1}{2}$ in. square cross-section. Diaphragm breaking time has been measured and found to be consistent with the observations on the shock formation distance.

1. INTRODUCTION

A number of investigators have shown that calculations of expected shock-tube performance based upon the usual ideal model of shock-tube flow (i.e. no attenuation, instantaneous diaphragm removal, and one-dimensional flow) agree satisfactorily with experiment, the observed shock being slightly weaker than predicted for the given initial conditions. Even the effect of a change in area at the diaphragm section has been shown to be amenable to a one-dimensional treatment (Alpher & White 1958). Most of the reported comparisons between expected and observed shock-tube performance, however, have concerned relatively weak shocks generated by diaphragm pressure ratios less than $\varkappa \equiv p_4/p_1 = 10^3$ (for example, Bleakney, Weimer & Fletcher 1949). With a $\varkappa$ of the order of 10^4, shocks stronger than predicted were observed and reported without comment by Yoler (1954) and Rabinowicz (1957). One might expect that the greater

velocity, temperature and pressure ratios encountered as stronger shock waves are generated would cause greater departures from the expected performance, and that study of these departures might illuminate the nature of real shock-tube flows.

Previous investigators have demonstrated photographically (Geiger & Mautz 1949; Glass, Martin & Patterson 1953) that the process by which a diaphragm actually ruptures involves formation of a small opening near the centre, followed by the outward tearing of the material and the folding back of the leaves so formed. The effective cross-sectional area of the shock tube at the diaphragm location therefore increases gradually with time instead of attaining its maximum value instantaneously as assumed in the usual ideal analysis. The effective piston velocity pushing on the driven gas increases with the degree of opening of the diaphragm. Since each positive increment in this piston velocity sends out a compression wave, the gradual opening will generate a train of compression waves which must overtake each other to form a shock wave. Further, the high velocity jet which issues from the first hole in the diaphragm generates a high degree of turbulence as it penetrates the driven gas; and as the contact zone between the driver and driven gases moves down the tube, the initially gross mixing proceeds toward mixing on a microscopic scale. These two processes resulting from the gradual diaphragm removal, generation of a large amplitude steepening compression wave and the mixing of the driver and driven gases, will be examined more closely to determine what observable effects might be expected to result.

2. Theory

Formation of a shock from a compression wave

To estimate the result of a finite but unspecified opening time for the diaphragm, consider that an unsteady isentropic compression wave is first formed in the driven gas, and that the pressure profile of this compression wave then steepens as it progresses down the tube so that a shock wave is formed. Since the gas velocity is not the same behind a shock wave as behind a compression wave having the same pressure ratio, a third reflected wave is required to match the boundary conditions as the shock is formed. It is readily shown that this third wave must be an upstream-facing expansion wave, and that the transmitted shock wave has a lower pressure ratio than does the original compression. To determine the expected shock-tube performance as a function of the diaphragm pressure ratio, the pressure and velocity of the expanded driver gas (p_3, u_3) will be equated to the pressure and velocity behind the compression wave (p_c, u_c); and then the strength shock (p_2/p_1 or u_2/a_1) resulting from the steepening of this compression wave will be determined. This model of the shock-tube flow is displayed in the (p, x, t)-diagram of figure 1. Since further wave reflections and interactions are not taken into account, the strength computed on this basis must represent a transient condition. The shock strength

should approach that predicted from the usual model (neglecting losses) as the effects of the starting process disappear.

For simplicity in the analysis required to determine the shock formed from a given compression wave, consider that the individual elements of the compression all overtake the leading edge at the same point in the tube, resulting in a transmitted shock and a reflected expansion fan as shown in figure 1 and the insert of figure 2. Let the state of the gas in

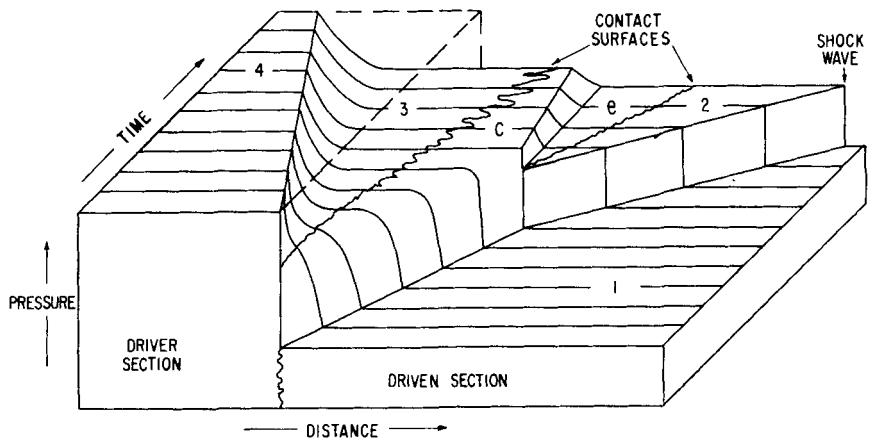

Figure 1. Suggested model of shock-tube flows as depicted by a (p, x, t)-diagram.

the various regions be indicated by the suffixes 1, 2, c, and e. In figure 2, for $\gamma_1 = 1{\cdot}4$, the curve labelled 'isentropic compression' represents the locus of states which may be reached through an isentropic unsteady compression wave from the initial state $(p_1, u_1 = 0)$ assuming ideal gas properties. Similarly, the curves labelled 'shock states' represent the locus of states (p_2, u_2) which may be reached from the initial state through a shock wave, assuming ideal gas properties or equilibrium air, as indicated. From any selected state (p_c/p_1) on the compression curve, the locus of states which may be reached through a backward-facing unsteady isentropic expansion wave (again assuming ideal gas properties) may be constructed as has been done to obtain the dashed lines labelled 'expansions'. The intersection of such an expansion curve with the shock curve determines that gas state which can satisfy the boundary conditions $p_e = p_2$ and $u_e = u_2$, and hence defines the shock which will result from the steepening of the initial compression.

When the driver and driven gases have been selected, and the sound velocities a_1 and a_4 and specific heat ratios γ_1 and γ_4 are known, then from the velocity ratio u_c/a_1 behind the selected compression wave p_c/p_1, the value of u_3/a_4 is determined by the requirement that the velocities be matched across the contact surface, $u_3 = u_c$. From u_3/a_4 the expansion pressure ratio p_4/p_3 for the driver gas is found, assuming as usual that $u_4 = 0$. The

diaphragm pressure ratio is then determined from $(p_4/p_3)(p_c/p_1) = x$. The procedure for obtaining the expected shock-tube performance curve based on the ideal model with instantaneous diaphragm removal is well known.

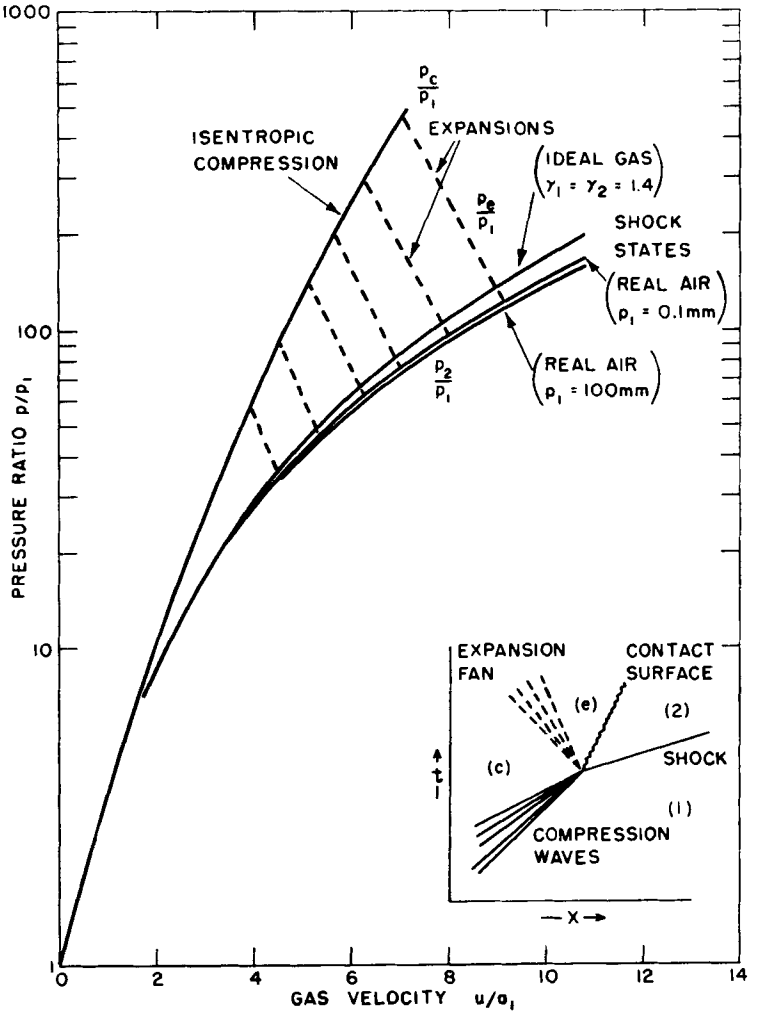

Figure 2. A graphical method for determination of the strength of the shock wave formed by steepening of an isentropic compression wave; $\gamma_1 = 1{\cdot}4$.

For the large diaphragm pressure ratios considered here, the gases cannot in general be considered ideal for either model of the shock-tube flow. Equilibrium shock Hugoniots for the shocked gases were used and were obtained from the following sources: for air, Gilmore (1955); for nitrogen and oxygen, Alpher & Greyber (1958); and for argon, Bond (1954) and unpublished calculations supplied by AVCO Research

Laboratory. In addition, hydrogen used as a driver gas expands to such low temperatures that changes in the degree of excitation of its internal degrees of freedom must be considered (Huber 1958). It may be noted that use of the equilibrium isentrope (Hilsenrath 1955) for the hydrogen expansion results in a decrease by about one Mach number in the predicted shock strengths for $\varkappa \sim 10^6$, this decrease being greater for the ideal model because of the larger expansion ratio.

Expected performance curves for the various gas combinations are given in figures 3 to 7, both for the ideal model and for the 'formation-from-compression' model for a shock tube with an area reduction of 1·51 across the diaphragm section. The method of Alpher & White (1958) is useful when equilibrium gas properties are to be incorporated.

It is characteristic of the flow processes associated with this formation-from-compression model that the initial rate of extraction of energy from the driver gas is lower than that rate obtained using the ideal model. That is, for a given diaphragm pressure ratio the driver gas expands through a smaller pressure ratio and acquires a lower velocity. Yet in some instances a stronger shock is predicted. This seeming contradiction is associated with the transient nature of the flow being analysed. We have considered in this model an isentropic compression wave whose leading edge propagates at the velocity of sound a_1 in the low pressure gas. Although energy has been extracted from the driver at a lower rate, up to the point where the shock forms this energy has gone isentropically into a quantity of gas proportional to a_1, whereas in the ideal model the energy goes anisentropically into a quantity of gas proportional to the product of the shock Mach number and a_1. When the transmitted shock forms from this compression, it is maintained both by the energy still being taken from the driver gas through the first expansion wave (state 4 to state 3) and by the additional energy extracted from the isentropically compressed driven gas through the second upstream-facing expansion wave (state c to state e). This region of driven gas which has undergone an isentropic compression acts in a sense as an energy accumulator, feeding energy back to generate transiently a shock wave stronger than can be maintained by the energy being taken from the driver gas alone.

This formation-from-compression model can be only an approximation, of course, because moderately strong shocks are found relatively near the diaphragm even when the maximum strength occurs much further down the tube. Since the entropy rise across a shock wave is proportional to the cube of the shock strength, however, this isentropic model should be a reasonable approximation even if, for example, a series of weaker shocks overtake each other to form a strong shock.

Mixing of gases in the contact region

It is clear that during every shock-tube experiment the driver and driven gases mix to some extent. While the magnitude of such mixing must be influenced by many factors, including the gases used and the shock strength,

a jagged opening projecting into the tube (the breaking diaphragm) would in particular promote mixing. While a quantitative prediction of the effect of such mixing on the shock strength cannot be made, nevertheless the direction of the effect may be determined.

In those experiments where the driver and driven gases have different heat capacities, this mixing if considered to be carried forward at constant pressure will be accompanied by a change in volume, since the gases will generally be at different temperatures. While this change in volume is taking place, there is effectively a velocity gradient across the region of mixing resulting in unequal velocities for the regions of uniform flow on either side. To indicate the direction and possible magnitude of this change in volume, consider on either side of an ideal contact surface two equal volumes $\frac{1}{2}V$ containing n_a moles of gas a at temperature T_a and n_b moles of gas b at T_b, respectively. Let $N = T_a/T_b = n_b/n_a$. The change in volume after mixing has been completed at constant pressure is obtained from

$$1 + \frac{\Delta V}{V} = \frac{1+N}{2}\left(\frac{1 + C_{p_a}/C_{p_b}}{N + C_{p_a}/C_{p_b}}\right),$$

and for $N \gg 1$, this becomes $\frac{1}{2}(1 + C_{p_a}/C_{p_b})$.

Considering only shock-tube experiments where the driver and driven gases are initially at the same temperature (not combustion driving), a region of the flow which includes the contact zone would be expected to undergo a volume increase from the mixing of a monatomic driver gas and a diatomic driven gas. Conversely, a volume decrease would be expected when the heat capacity of the driven gas is smaller than that of the driver gas. This mixing can be considered to affect the shock strength either through generation of pressure waves or through a change in the effective piston velocity. To give a numerical example, in a shock tube of constant bore, a diaphragm pressure ratio of 10^4 between helium and air would produce on an ideal basis a Mach 7 shock. The temperature of the expanded helium would be 38° K, and that of the shocked air 3140° K. This yields $N = 83$, and $\Delta V/V = 0{\cdot}194$. The limiting value for large diaphragm pressure ratios for these gases is $\Delta V/V = 0{\cdot}20$.

The effect on the shock wave cannot be determined quantitatively, since one does not know either the extent of the mixing region or the rapidity with which mixing approaches completion; and hence neither the magnitude of the compression waves nor the difference in flow velocity across the contact zone is known. It may further be pointed out that with the stronger shock waves the excitation of further internal degrees of freedom of the shocked gas results in a still greater heat capacity, and hence a greater value for the strong shock limit of $\Delta V/V$. Wray (1956) has reported observations on strong shock waves ($M_s \sim 8$) generated in fluorine by use of helium as a shock-tube driver gas. Fluorine is largely dissociated under these conditions and hence has a large heat capacity. He observed the shock velocity first to decrease with increasing distance from the diaphragm, reach a minimum, and then increase to the end of the tube.

Effect of diaphragm opening time on formation distance

The expected effect of the diaphragm opening time upon the formation distance may also be estimated by use of a simple model. Assume first that in a shock tube of constant bore the flow at any time is that predicted by use of the ideal model, i.e. with instantaneous diaphragm removal. Let the gas combination and the diaphragm pressure ratio be given, and further assume ideal-gas behaviour for both driver and driven gases. Then one determines the distance travelled by the shock wave at the time it is overtaken by a sound wave originating from the diaphragm location at some given time after the flow was initiated. This distance becomes relevant if one assumes that the maximum shock strength occurs as a result of the last compression sent out as the diaphragm is fully removed.

Proceeding downstream from the diaphragm location, the flow may be divided into three regimes, an upstream-facing, isentropic unsteady expansion wave, a region of uniform flow of expanded driver gas, and a region of uniform flow of shocked gas. The velocity of propagation of a sound wave will be the sum of the fluid velocity and the local velocity of sound. Assume for simplicity that the average velocity of propagation through the unsteady expansion wave is the mean of the velocities at the diaphragm location and at the foot of the expansion wave. All flow velocities, local sound velocities and propagation velocities may be readily calculated on this basis. A consequence of the highly idealized model utilized is that the distance travelled by the shock will be directly proportional to the time after flow initiation at which the signal is sent out. Representative results are given in table 1.

Gases	Diaphragm pressure ratio	Shock Mach number	Formation distance per 100 microseconds effective diaphragm opening time
He/N_2	2500	6	6·5 ft.
H_2/N_2	2500	8·8	8·3 ft.
H_2/N_2	334	6	3·3 ft.

Table 1. Estimation of formation distance for finite opening time of diaphragm.

It may be noted from table 1 that, for the same shock strength, the shock should form in only half the distance with a hydrogen driver as compared with a helium driver. For the same diaphragm pressure ratio, the formation distance with the hydrogen driver is only 30% greater. The use of a combustion driver would further shorten the formation distance for a given shock strength, because of the higher temperature and hence higher propagation velocity through the expanded driver gases.

3. Experiments

Apparatus and procedure

These data were obtained in the 3·25 in. square shock tube at the General Electric Research Laboratory. The driver section of this tube is of 4·5 in. inside diameter and 6·5 ft. long, and the driven section is 3·25 in. square and 42 ft. long. Most of the diaphragms used in these experiments were made of type 302 stainless steel, 0·018 in. thick, scored in the form of an X by a milling cutter with a 0·010 in. radius tip. The groove depth was generally 0·008 or 0·009 in., and the breaking pressures varied from 15 to 30 atm. The unsupported diameter was 4·5 in.

For most of these experiments the initial pressure in the driver section was between 0·040 and 10 mm of mercury, and was recorded as the average of the readings of two McLeod gauges or, for the higher pressures, a precision Bourdon gauge. A calibrated Bourdon gauge was used to read the driver gas pressure as it was slowly increased to the point of rupture of the diaphragm. From these readings the pressure ratio across the diaphragm was obtained as the independent variable.

The arrival of the shock wave at each of up to twelve stations along the tube caused a signal to be displayed on a cathode-ray oscilloscope which was tracing a raster pattern at the rate of 20 microseconds/cm. A photographic record of the trace permitted determination of the variation of shock velocity with distance from the diaphragm. The transducers employed in the tube were thin-film heat gauges, ionization gauges, or pressure gauges of our own design, depending upon the conditions of the experiment; and they were typically 32·6 in. apart.

The average shock Mach number was computed for the interval between each pair of shock detection stations, and the maximum of this set of values plotted against the diaphragm pressure ratio.

Shock tube performance curves

Experimental shock-tube performance data together with predicted curves are shown in figure 3 for helium/nitrogen and hydrogen/nitrogen, and in figure 4 for helium/argon and hydrogen/argon. The tendency for the experimental points to follow the formation-from-compression curve is clear, and in fact shocks stronger than predicted by the ideal model are noted for all gas combinations. For the case of helium/nitrogen in figure 3, as well as helium/oxygen in figure 5 and helium/air in figures 6 and 7, the shock strengths exceed even the stronger of the two predicted curves. These gas combinations are such that one would expect the contact zone mixing to enhance the shock strength. For hydrogen/argon, where the mixing would be expected to attenuate the shock, the experimental points are somewhat weaker relative to the compression-formation curve than are the hydrogen/nitrogen data. For helium/argon and hydrogen/nitrogen, mixing should have no effect to the extent that further excitation of internal degrees of freedom may be neglected.

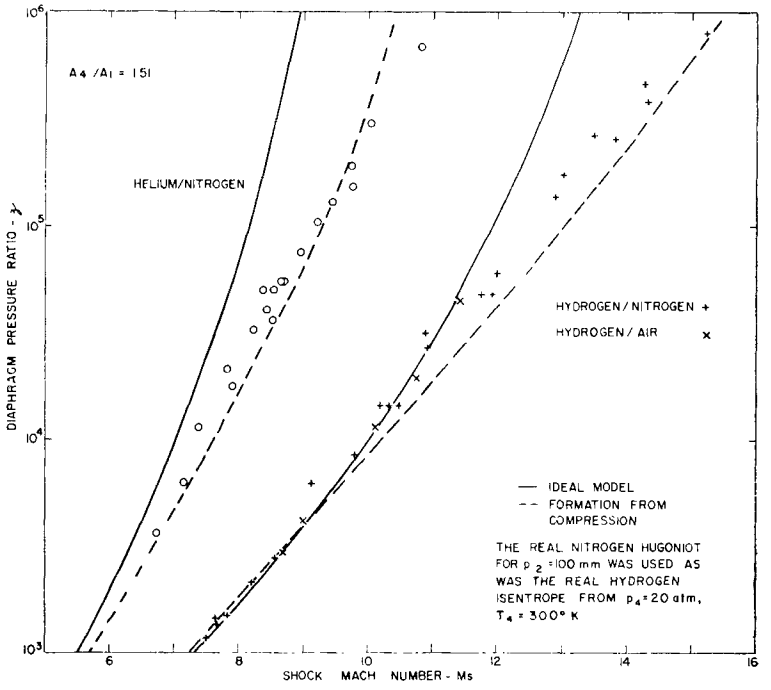

Figure 3. Observed and predicted shock-tube performance for helium/nitrogen and hydrogen/nitrogen. Experimental points indicate the maximum strength observed in an experiment. Compression waves due to contact zone mixing would enhance the shock strength for helium/nitrogen.

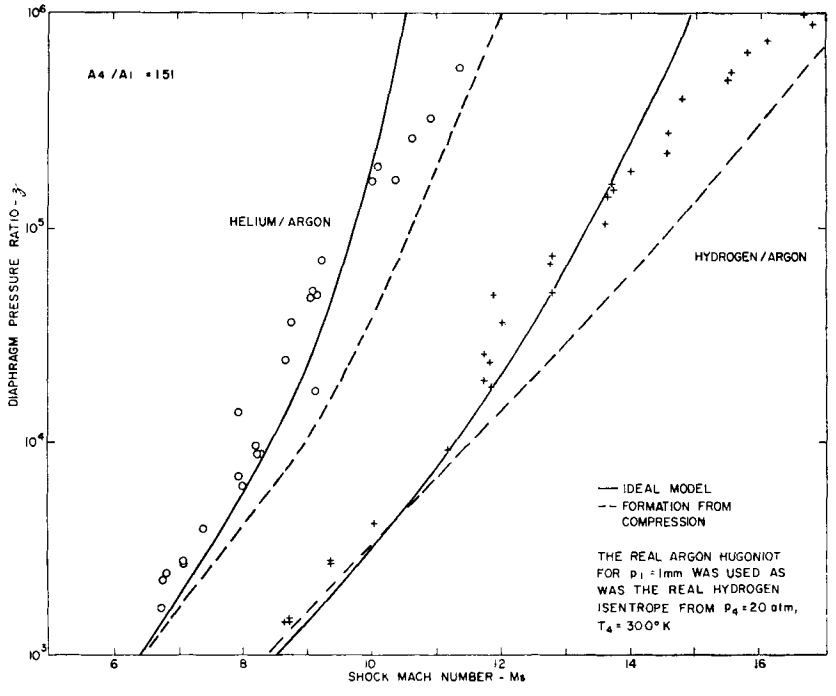

Figure 4. Observed and predicted shock-tube performance for helium/argon and hydrogen/argon. Expansion waves due to contact zone mixing would weaken the shock in hydrogen/argon experiments.

A set of experiments was run with helium/oxygen to determine whether significant differences could be found relative to helium/nitrogen. For the strongest shocks ($M_s \sim 10$), the dissociation of the oxygen is significant whereas it is still negligible for nitrogen; and the heat capacity, and hence the effect of mixing with the helium, would be greater for oxygen than for nitrogen. The data are given in figure 5. Comparison with the helium/nitrogen results given in figure 3 shows that the helium/oxygen shocks appear to be somewhat stronger.

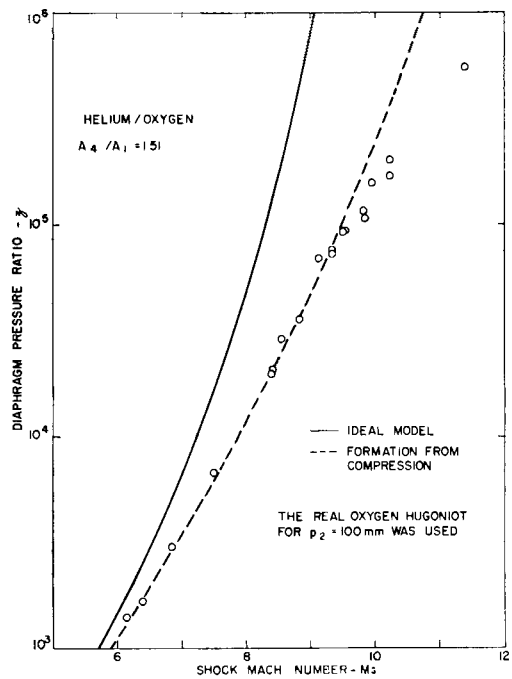

Figure 5. Observed and predicted shock-tube performance for helium/oxygen.

The data shown in figure 6 were obtained in connection with work on the effect of an area ratio across the diaphragm section (Alpher & White 1958). These experiments show that the incremental shock strength due to a change in the area ratio across the diaphragm section is adequately predicted by a theory based on the ideal model even though the actual shock strength may be appreciably greater than predicted.

Use of the equilibrium rather than the ideal-gas Hugoniot for the shocked gas results in the prediction of a weaker shock for a given diaphragm pressure ratio. Expected performance curves have been computed both on the basis of an ideal gas and of a real gas, and the comparison with experiment is shown in figure 7 for helium/air. The rather striking agreement with the real-gas compression-formation curve is probably partially fortuitous, in

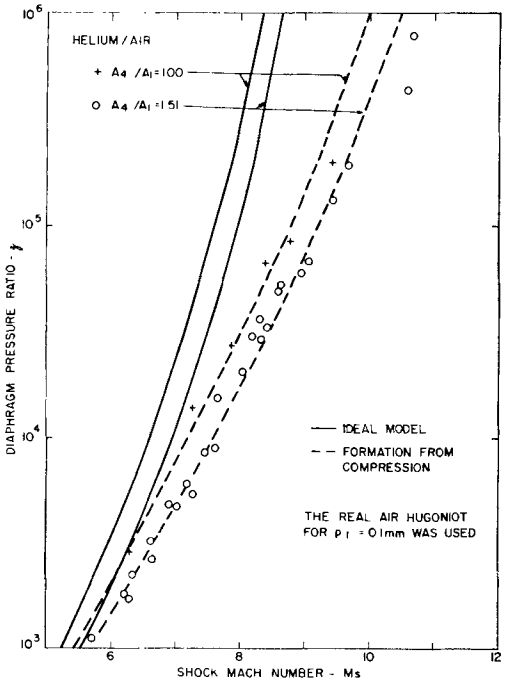

Figure 6. The effect of an area ratio across the diaphragm section upon the maximum shock strength observed.

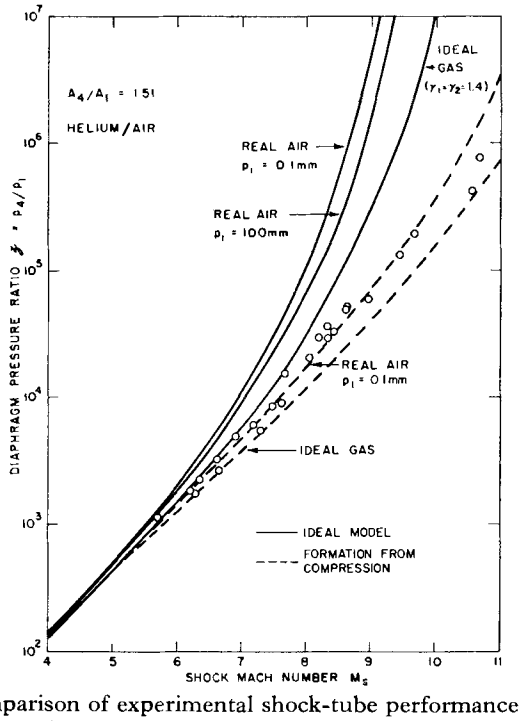

Figure 7. Comparison of experimental shock-tube performance with predicted performances based upon various assumptions.

the sense that apparently the enhancement effects of mixing approximately balanced the attenuation mechanisms which must always be present.

In each of figures 3 to 7, the shock strengths observed for the largest diaphragm pressure ratios represent a lower bound on the maximum which could have occurred in the experiments, since the shock was still accelerating at the end of the tube where the recorded strength was measured.

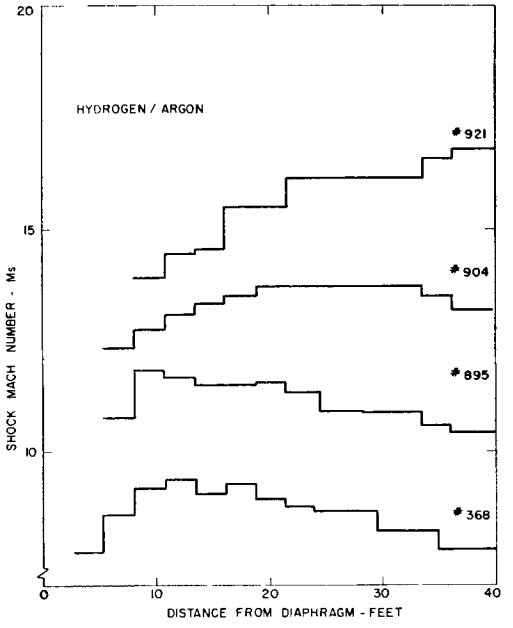

Figure 8. Typical records of shock strength at various distances from the diaphragm in the $3\frac{1}{4}$-in. square shock tube. The horizontal lines indicate the average velocity of the shock wave over the corresponding distance. For the largest diaphragm pressure ratios the shock is still accelerating at the end of the tube.

Further indication of the relative magnitudes of the mixing and formation-from-compression effects may be noted from the shock velocity records. In the hydrogen/argon experiments, for example, in addition to the losses due to the interaction between the shocked gas and the wall, the mixing at the contact surface would, for the weaker shocks, cause the shock to decelerate. The attenuating effect of mixing would decrease, however, for the stronger shocks when the hydrogen is cooled to the point that its heat capacity approaches that of a monatomic gas, and when the ionization of the argon greatly increases its heat capacity. Representative data showing the variation of shock strength with distance along the tube are given in figure 8. The horizontal lines indicate the average velocity of the shock over the corresponding distance, and do not imply that the actual shock velocity varied in a stepwise fashion. For the larger diaphragm pressure ratios, the shock wave is observed to accelerate for the full length of the tube, emphasizing the dominant role played by these non-ideal processes.

From such velocity records the distance along the tube required for realization of the maximum shock strength has been determined. This distance is plotted *vs* shock Mach number in figure 9, and *vs* diaphragm

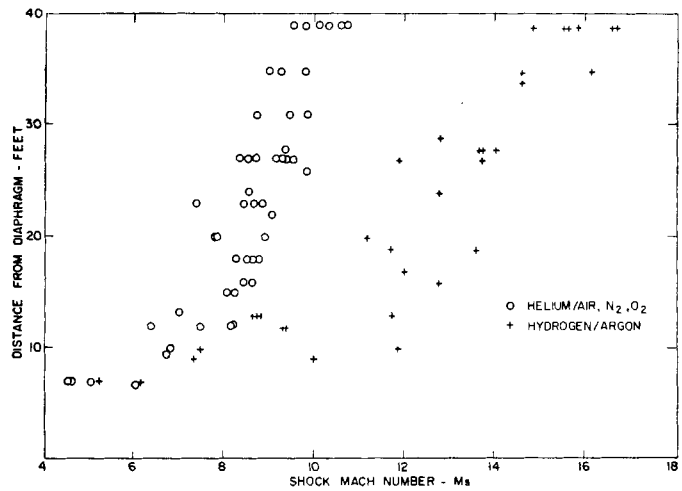

Figure 9. Shock-formation distance as a function of shock Mach number in the $3\frac{1}{4}$-in. square shock tube. Points for helium/argon and hydrogen/nitrogen generally lie between the helium/nitrogen and the hydrogen/argon values.

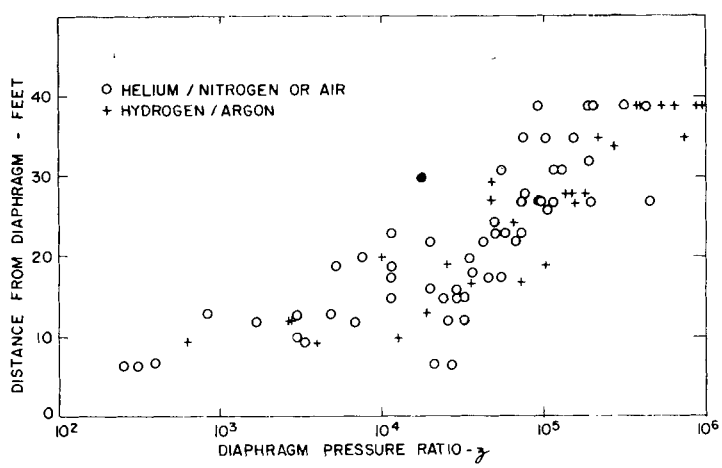

Figure 10. Shock-formation distance as a function of diaphragm pressure ratio in the $3\frac{1}{4}$-in. square shock tube, Points for helium/argon and hydrogen/nitrogen are similarly distributed. The solid point was obtained by loading each of the four leaves of the scored diaphragm with 6·2 gm of solder.

pressure ratio in figure 10. The curves probably apply only to this particular tube and to these diaphragms, and should be used only qualitatively in estimating the expected performance of other shock tubes.

Diaphragm opening time

To determine experimentally the time required for the leaves of the diaphragm to fold back to the full open position, the transmission of light through the diaphragm section was measured as a function of time. A light source was mounted near a $\frac{3}{8}$ in. window in a blind flange at the end of the driven section, 42 ft. from the diaphragm. A barium titanate pressure transducer was mounted in the driver chamber wall near the diaphragm section and responded to the metal vibration as the diaphragm first began to break under the gradually increasing pressure, producing a signal to trigger a cathode-ray oscillograph. A photomultiplier viewing the side wall of the driven chamber observed the variation with time of the intensity of the scattered light and displayed it on the oscillograph.

The diaphragms used in these experiments took about 600 microseconds to open fully. The initial rate of opening was low however, since the light intensity recorded had reached less than 10% of its final value after 200 microseconds. This slow initial rate of opening was also characteristic of both 0·010 in. and 0·035 in. thick diaphragms, which took somewhat shorter and longer times respectively to open fully.

These measurements of formation distance and diaphragm opening times are considered to be consistent with the highly simplified analysis previously described, since the many approximations involved preclude other than qualitative interpretation of the results. For example, a convergence at the diaphragm section would tend to shorten the formation distance because of the higher temperature of the expanded driver gas, and attenuating effects would do likewise by inhibiting attainment of the maximum possible shock strength.

However, one may conclude that an opening time of several hundred microseconds should result in an appreciable formation distance for the larger diaphragm pressure ratios, and that this distance should be more nearly independent of diaphragm pressure ratio than of shock Mach number as various gases are used. This is observed in figures 9 and 10.

Shock attenuation

Since these stronger-than-predicted shock waves (as in helium/nitrogen) exist only transiently, successive wave interactions may be expected to reduce the shock strength. Mixing in the contact zone may either have no effect or act to enhance or reduce the shock strength, depending upon the gases employed. Therefore, these two effects associated with the starting of the shock tube flow may both strengthen and 'attenuate' the shock at different times in the same experiment. Interpretation of attenuation data from strong-shock experiments in terms of energy loss mechanisms must be done carefully, since these other adiabatic processes may also cause the shock strength to vary with time.

4. Conclusions

The finite time required for removal of the diaphragm can result in an appreciable modification of the shock-tube flow for the case of the larger diaphragm pressure ratios. For a monatomic driver/diatomic driven gas combination, this opening time can cause generation of a shock significantly stronger than predicted by the usual model. An analysis based upon the formation first of a compression wave, then of a shock wave, agrees with experiment. The mixing of the driver and driven gas in the contact zone may also modify the shock strength, either strengthening or weakening it according to the relative heat capacities of the gases used. Observed shock deceleration may result partially from these adiabatic processes of mixing and wave interactions, as well as from attenuating effects of energy losses to the wall.

The shock-tube starting process can occupy a significant portion of the length of the tube. In these experiments, for the largest diaphragm pressure ratios ($\bar{x} \sim 10^6$) the shock was still accelerating 40 ft. from the diaphragm.

The one-dimensional analysis of Alpher & White (1958) successfully predicts the shock enhancement due to area ratio at the diaphragm, even for the larger diaphragm pressure ratios where the actual shock strength may not be predicted by use of the ideal model.

In experiments employing combustion driving, approximately equivalent performance curves are computed from the ideal model, whether hydrogen or helium is employed as a diluent. The processes discussed here, however, might cause one or the other to be advantageous in a particular experiment.

This research was supported by the Ballistic Missile Division of the United States Air Force under contract AF-04-(645)-24. A preliminary account of the work was given at the annual meeting of the American Physical Society in New York, January 1957.

References

Alpher, R. A. & Greyber, H. D. 1958 *General Electric Research Lab., Schenectady, Rep.* no. 58–RL–1915.

Alpher, R. A. & White, D. R. 1958 *J. Fluid Mech.* **3**, 457.

Bleakney, W., Weimer, D. K. & Fletcher, C. H. 1949 *Rev. Sci. Inst.* **20**, 807.

Bond, J. W. 1954 *Los Alamos Scientific Lab. Rep.* no. LA–1693.

Geiger, F. W. & Mautz, C. W. 1949 *University of Michigan, Engr. Res. Inst. Rep., Proj.* M 720–4.

Gilmore, F. R. 1955 *Rand Corporation Rep.* no. RM–1543.

Glass, I. I., Martin, W. & Patterson, G. N. 1953 *Institute of Aerophysics, University of Toronto, UTIA Rep.* no. 2.

Hilsenrath, J. 1955 *Nat. Bur. Stand., Wash., Circular* no. 564.

Huber, P. W. 1958 *J. Aero. Sci.* **25**, 269.

Rabinowicz, J. 1957 *California Institute of Technology, Guggenheim Aeronautical Lab., Hypersonic Wind Tunnel Project, Mem.* no. 38.

Wray, K. L. 1956 Ph.D. Thesis, Brown University.

Yoler, Y. A. 1954 *California Institute of Technology, Guggenheim Aeronautical Lab., Hypersonic Wind Tunnel Project, Mem.* no. 18.